



Effects of Post Weld Heat Treatment on Mechanical and Electrochemical Properties of Welded Carbon Steel Pipe

Jeong-Hun An¹ · Jihoon Lee¹ · Yong-Sang Kim¹ · Woo-Cheol Kim² · Jung-Gu Kim¹

Received: 13 May 2018 / Accepted: 30 September 2018 / Published online: 26 October 2018
© The Korean Institute of Metals and Materials 2018

Abstract

To prevent a failure caused by stress corrosion cracking (SCC) of welded carbon steel pipe in district heating systems within service life, the effects of post weld heat treatment (PWHT) on the mechanical, electrochemical properties and resistance of SCC were investigated. As the result of normalized treatment, Vickers hardness, yield strength and tensile strength decreased, but ductility increased. Electrochemical properties were evaluated using potentiodynamic polarization tests and electrochemical impedance spectroscopy. Uniform corrosion was observed on all specimens, although the corrosion rate was slightly increased by PWHT. The resistance of SCC was evaluated using slow strain rate test under the accelerated corrosion condition. The resistance of SCC was increased by PWHT, especially by normalized treatment. If the reduced strength by PWHT satisfies the design stress, it is possible to decrease the probability of failure within service life in welded pipeline by normalized treatment.

Keywords Metals · Heat treatment · Microstructure · Corrosion · Mechanical properties

1 Introduction

District heating systems are energy utilities that provide heat to remote customers from centralized sources [1]. District heating has many advantages, including safety, convenience, and reduction of costs by avoiding the need for heating equipment to be installed in each individual building or household [2]. Various materials have been used in district heating pipelines [3]. One of the most frequently used materials is carbon steel pipe, due to its strength, availability and low cost [4–9].

In addition to its advantages, carbon steel pipe also has disadvantages, including cracking, fatigue, and corrosion problems in the weld zone. Welding is commonly used for construction of long-distance district heating pipelines [10]. When carbon steel pipe is welded, the microstructures of the weld zone and heat affected zone (HAZ) differ from those of the base metal [11–13]. These different microstructures

result in large variations in strength across the weld joints and cause electrochemical dissimilarity of individual parts in the weldment, which induces corrosion between base metal-weld zone couples exposed to corrosive environments [14, 15].

To improve the performance of the weld zone and to reduce the residual stress of the HAZ, PWHT are often used [11]. PWHT include stress relieving, process annealing, and normalizing treatments; each is conducted at an appropriate temperature [16] that depends on the carbon content in the steel. Commonly, the effect of PWHT on hydrogen embrittlement (HE) properties of the welded steel was investigated because it was used to reduce the potential for HE [17–19]. Kim and Lee [20] investigated the mechanical properties in the PWH-Treated HAZ of steel welds. Moon [21] investigated the corrosion resistance affected by PWHT on HAZ. However, the effect of PWHT on stress corrosion cracking (SCC) properties was estimated by few studies. SCC in weld metal and HAZ was one of the major causes of the failure in carbon steel pipes that widely used for water and gas transmission. It was a progressive fracture result of the combined influence of tensile stress and corrosive environment [22]. To prevent the failure of carbon steel pipes, research on the effects of PWHT on mechanical, electrochemical properties and the resistance of SCC would be necessary. Moreover,

✉ Jung-Gu Kim
kimjg@skku.edu

¹ School of Advanced Materials Science and Engineering, Sungkyunkwan University, Suwon 16419, Republic of Korea

² Technical Efficiency Research Team, Korea District Heating Corporation, Yongin 06340, Republic of Korea

Table 1 Chemical composition of carbon steel pipe used in the district heating system

Elements	C	Si	Mn	P	S	Fe
Composition (wt%)	0.25	0.35	0.30–0.90	0.040	0.040	Bal.

Table 2 Welding procedure specifications

Welding process	Gas tungsten arc welding (GTAW)
Joint design	Single-V joint with a 65 ± 5 degree included angle and a 1.6 ± 0.8 mm root face
Number of passes	1–2 or higher
Electrode	ER70S-G (2.4 or 3.2 mm diameter, Thoriated, TGC-50)
Voltage	11–15 V or 22–28 V
Current	80–130 A or 100–170 A
Polarity	Direct current straight polarity (DCSP)
Travel speed	5–10 cm/min or 6–16 cm/min
Welding atmosphere	Argon, 7–17 L/min

many studies have addressed the effects of PWHT on the mechanical properties and corrosion behavior of stainless steel pipe previously, but few studies have focused on carbon steel pipe.

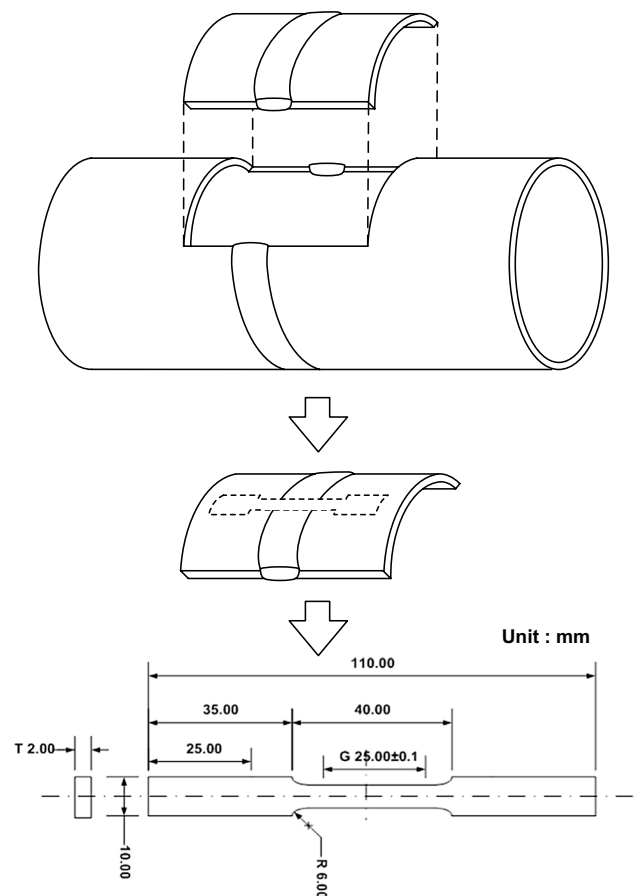
This study evaluated the mechanical and electrochemical properties of weld joint of carbon steel pipe after PWHT performed at various temperatures. Mechanical properties were evaluated by hardness tests, tensile tests. And, potentiodynamic polarization and EIS tests were carried out to characterize corrosion behavior of the carbon steel pipe weldment. Finally, the resistances of SCC in district heating systems were evaluated by slow strain rate test (SSRT) in the synthetic district heating water with the anodic potential that accelerates the corrosive condition.

2 Experimental Procedures

2.1 Specimen and Solution Preparation

The specimen used in the study was a carbon steel pipe in district heating systems; its chemical composition is shown in Table 1, and the detailed welding process is described in Table 2. After welding, sectioning procedures were carried out to prepare SSRT specimens from welded pipes as shown in Fig. 1.

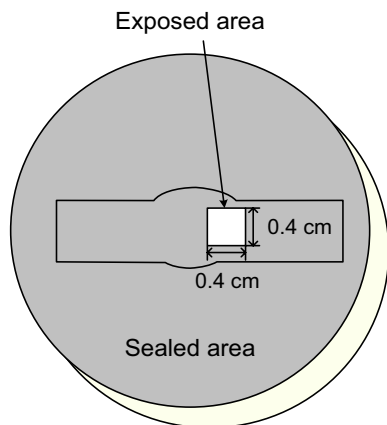
For the electrochemical test, the surface of the specimen was abraded with 600-grit silicon carbide (SiC) paper, rinsed ultrasonically with ethanol and finally dried in air. Table 3 gives the chemical composition of the synthetic district heating water. De-aerated synthetic district heating water at 80 °C and pH of 9.0 was used as the corrosion medium. Specimens were heated at a specified rate to the temperature

**Fig. 1** Schematic illustration of the sectioning procedures used to prepare SSRT specimens from welded pipes

of the stress relieving heat treatment (595 °C) and normalizing treatment (900 °C), held for 4 h, and then air-cooled.

Table 3 Chemical composition of the synthetic district heating water (mg/L)

pH	FeCl ₃	NaNO ₂	NaNO ₃	NaCl
9.0	16.25	7.5	0.7	65.2

**Fig. 2** Schematic illustration of weldment and exposed area of the specimen

2.2 Microstructure Observation

To investigate the effects of PWHT on welded carbon steel pipe, microstructures were observed. The specimens were ground with SiC paper to 2000 grit, and then polished using diamond paste down to 1 μm . After that, the specimens were etched with a 2% nital etchant for 10 s. Microstructures of weldment areas were then observed using a Leica DM2700 M optical microscope (OM).

2.3 Electrochemical Measurements

The potentiodynamic polarization tests were carried out to evaluate corrosion behavior using a conventional three-electrode cell, with the test specimen as the working electrode, a saturated calomel electrode (SCE) as the reference electrode, and graphite as the counter electrodes, as shown in Fig. 2. The exposed area of the specimen from the weld metal to the base metal was $0.4 \times 0.4 \text{ cm}^2$. This test was conducted in accordance with American Society for Testing and Materials (ASTM) G5 using a Model VSP-300 (Biologic) potentiostat. A stable potential (Open-Circuit Potential, OCP) was established within 6 h in order to carry out the electrochemical test. After that, the polarization test was performed at a scanning rate of 0.166 mV/s from $-250 \text{ mV}_{\text{OCP}}$ to $+1000 \text{ mV}_{\text{SCE}}$.

EIS measurement was used to evaluate corrosion behavior using a conventional three-electrode cell. This test was conducted using a Model VSP-300 (Biologic) potentiostat at

open-circuit potential (OCP) with a sinusoidal amplitude of 10 mV in the frequency range from 100 kHz to 10 mHz. The impedance plots were interpreted on the basis of an equivalent circuit using a suitable fitting procedure by ZsimpWin software.

2.4 Mechanical Tests

The hardness of the carbon steel pipe weldment was measured using a Vickers hardness tester (Mitutoyo MVK-H2). The maximum load was adjusted to 200 g and the depth of indentation was automatically recorded in terms of arbitrary hardness numbers (HV). For the hardness test, the cross-section of the specimen was polished using a 9 μm diamond suspension. In total, 71 points were measured in each specimen, and the spacing between measured points was 0.1 mm.

2.5 Resistance of Stress Corrosion Cracking Tests

SSRT have been used extensively to evaluate the resistance of a material to environmentally induced cracking [23, 24]. In this study, SSRT was used to evaluate the effects of PWHT on the welded joint of the pipe. The load and strain were monitored continuously with a load cell and a linear variable differential transformer (LVDT) until fracture occurred. This test was conducted at a constant strain rate of $1.0 \times 10^{-5} \text{ s}^{-1}$. The three-electrode cell was also used to accelerate corrosion by supplying a constant potential of $-500 \text{ mV}_{\text{SCE}}$. A de-aerated synthetic district heating water solution was used. The fracture surface also was observed using a scanning electron microscopy (SEM).

3 Results and Discussion

3.1 Microstructure

Figures 3, 4 and 5 show the OM images of weld metal, HAZ and base metal of the welded carbon steel specimen for each applied PWHT. The as-welded specimen (a) and stress-relieved specimen (b) showed almost the same microstructures from the weld zone to the base metal in Figs. 3, 4, 5. A typical cast structure due to the high solidification rate was observed in the weld metal in Fig. 3. Although similar microstructures were observed in the HAZ and base metal, the grain size was larger in the HAZ due to heating effects. However, the normalized specimen had very different microstructures compared to the others. Polygonal ferrite structures were formed in all zones. However, the weld metal had dark particles (Fig. 3c) and the grain size decreased from the weld metal to the base metal in Figs. 3, 4, 5c respectively.

A typical microstructure was observed in the weld metal of the carbon steel pipe caused by an intermediate cooling

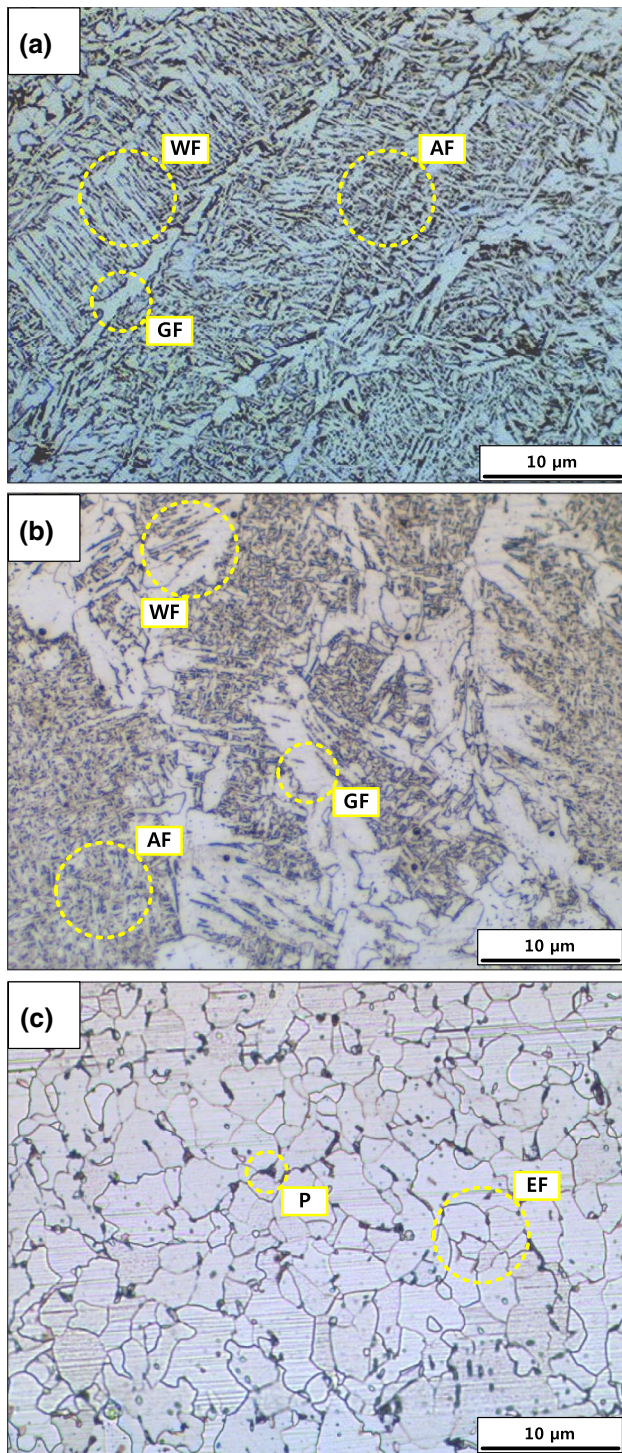


Fig. 3 Optical micrographs of the weld metal according to applied PWHT: **a** as-welded, **b** stress-relieved and **c** normalized

rate as the austenite transforms (Fig. 3a) [25]. The microstructure in the as-received specimen was composed of grain-boundary ferrite (GF), acicular ferrite (AF) and Widmanstatten ferrite (WF). The AF can be identified by lenticular plate structure that shaped and pointed like a needle.

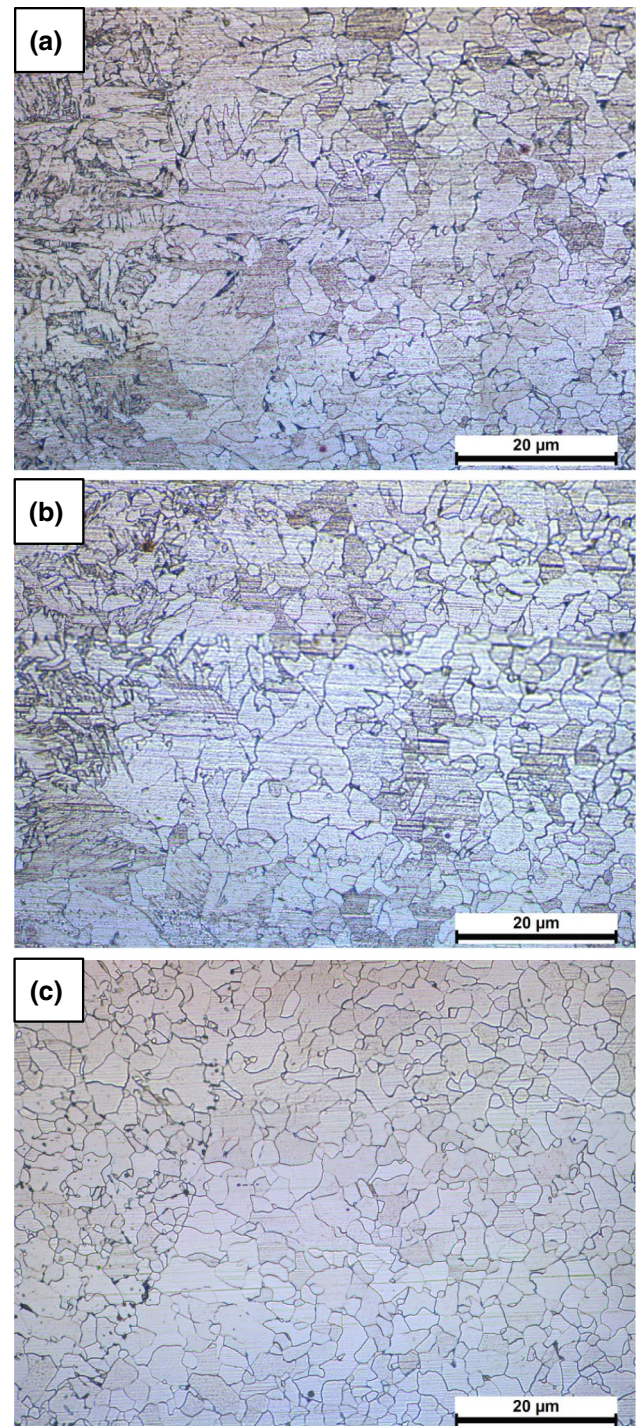


Fig. 4 Optical micrographs of the HAZ according to applied PWHT: **a** as-welded, **b** stress-relieved and **c** normalized

And the WF can be identified by ferrite plates which directly grow from the GF. Similarly, the microstructure of the stress-relieved specimen was composed of GF, AF and WF as shown in Fig. 3b. In contrast, the normalizing heat treatment changed the original as-received microstructure to an

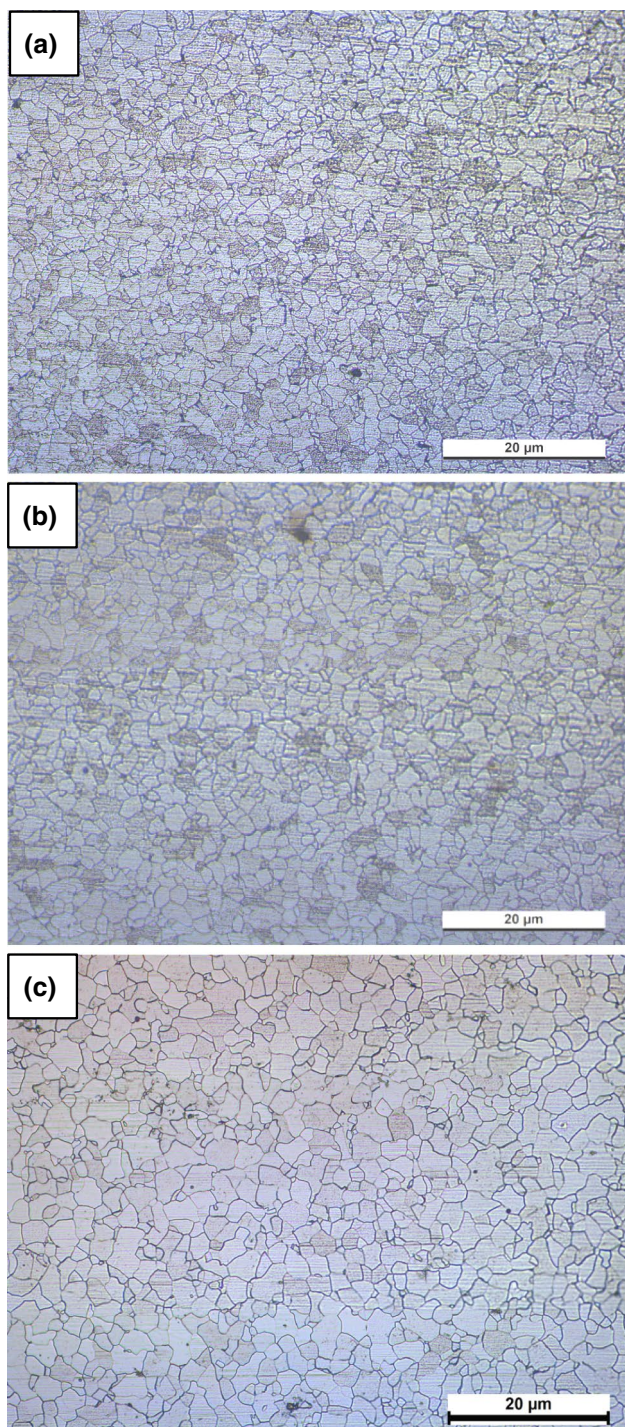


Fig. 5 Optical micrographs of the base metal according to applied PWHT: **a** as-welded, **b** stress-relieved and **c** normalized

equiaxed ferrite (EF) microstructure with very small pearlite (P) colonies as shown in Fig. 3c. The stress relieving heat treatment was conducted below the austenite transformation temperature, whereas the normalizing heat treatment was conducted above the austenite transformation temperature; this temperature difference influenced the microstructure

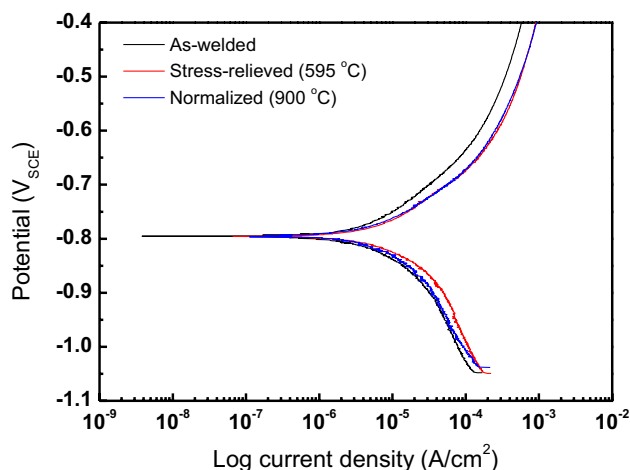


Fig. 6 Potentiodynamic polarization curves of the specimens in deaerated synthetic district heating water at 80 °C and pH of 9.0

difference between the stress-relieved and normalized specimens in weld zone.

Whereas the microstructure of the HAZ was not changed significantly by the stress relieving heat treatment (Fig. 4b) from the as-received specimen (Fig. 4a), a slight reduction in grain size was observed on the normalizing heat treatment specimen (Fig. 4c). Also, the microstructure of the base metal was not changed by the stress relieving heat treatment (Fig. 5b) relative to that observed on the as-received specimen (Fig. 5a), but the normalizing heat treatment increased grain size (Fig. 5c). These results were attributed to recrystallization and grain growth on the as-received specimen as a result of the normalizing heat treatment. Generally, grain size increases with increasing temperature of the heat treatment. These results indicate that the microstructure of the welded carbon steel pipe was not affected by the stress relieving heat treatment, but were affected by the normalizing heat treatment.

3.2 Corrosion Behavior

The potentiodynamic polarization test was conducted to investigate corrosion behavior of the welded carbon steel pipe. The corrosion current density (i_{corr}) was determined by the Tafel extrapolation method, and the corrosion rate can be inferred from the i_{corr} based on Faraday's law [22]:

$$\text{Corrosion rate (mm/year)} = \frac{0.00327 \times i_{\text{corr}} \times E.W.}{D} \quad (1)$$

where 0.00327 is the metric and time conversion factor, i_{corr} is the corrosion current density ($\mu\text{A}/\text{cm}^2$), E.W. is the equivalent weight (g) and D is the density (g/cm^3). Figure 6 shows the potentiodynamic polarization curves of welded carbon steel specimens (as-received, stress-relieved, and

Table 4 Results of potentiodynamic polarization test for the specimens in deaerated synthetic district heating water at 80 °C and a pH of 9.0

Specimens	E_{corr} (mV _{SCE})	i_{corr} (μA/cm ²)	β_a (V/decade)	β_c (V/decade)	Corrosion rate (mm/year)
As-welded	-789.851	7.275	0.137	0.172	0.085
Stress-relieved	-799.888	10.875	0.137	0.148	0.128
Normalized	-795.082	12.463	0.143	0.233	0.146

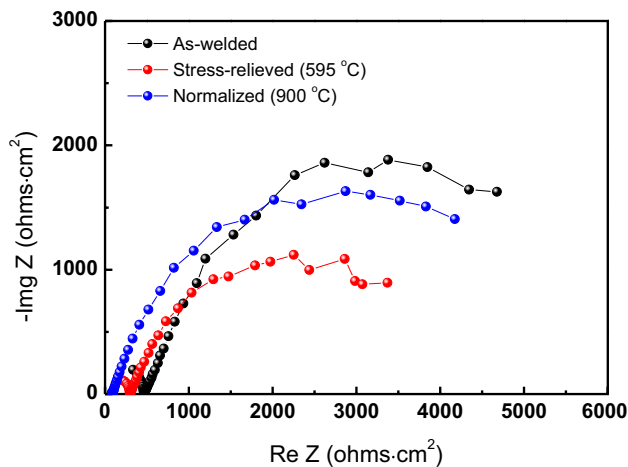


Fig. 7 EIS Nyquist plots of each specimen in deaerated synthetic district heating water at 80 °C and pH of 9.0

normalized) in the de-aerated synthetic district heating water at 80 °C and pH of 9.0. Also, Table 4 lists the calculated electrochemical parameters of the polarization curve. Corrosion potential (E_{corr}) was similar in all specimens and i_{corr} of the welded specimen was slightly increased after PWHT. Thus, the corrosion rate was slightly increased by PWHT, but the difference was not significant.

EIS test was conducted to investigate the electrochemical properties of the welded carbon steel pipe. Figure 7 shows EIS Nyquist plots of each specimen in the de-aerated synthetic district heating water at 80 °C and pH of 9.0. In the Nyquist plots, the diameter of the semi-circle is related to the polarization resistance (R_p) because the R_p is inversely proportional to i_{corr} according to the following equation:

$$R_p = \frac{\beta_a \times \beta_c}{2.3 \times i_{\text{corr}} \times (\beta_a + \beta_c)} \quad (2)$$

where β_a and β_c are the anodic and cathodic Tafel slopes, respectively. Thus, an increase in the radius of the semi-circle corresponds to a decrease in the corrosion rate. The one-time constant equivalent circuit shown in Fig. 8 was used for fitting the EIS data to obtain optimized resistance values, which are listed in Table 5. The impedance data is composed

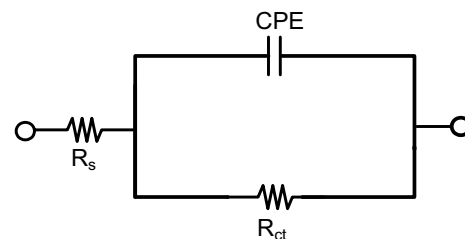


Fig. 8 Equivalent circuit for EIS fitting (one time constant)

Table 5 Impedance parameters of each specimen according to one time constant equivalent circuit

Specimens	R_s (Ω cm ²)	CPE		R_{ct} (Ω cm ²)
		C_{dl} (μF/cm ²)	n	
As-welded	468.0	577.5	0.702	6080
Stress-relieved	296.4	540.0	0.684	3720
Normalized	313.3	945.3	0.697	3676

of the following parameters: solution resistance (R_s), charge transfer resistance (R_{ct}), and constant phase element (CPE). CPE is the double layer capacitance formed by the electrical double layer that exists at the interface between an electrode and its surrounding electrolyte. The R_{ct} values of stress-relieved and normalized specimens decreased relative to the as-received specimen. Corrosion rates are expected to increase in the following order: as-received, stress-relieved, normalized specimen. Consequently, these results are consistent with those of the polarization curves, confirming that the corrosion rate was slightly increased by PWHT.

3.3 Mechanical Properties

Figure 9 shows the variation of the Vickers hardness (HV) values in relation to the distance from the center of the weld joint for the as-welded, stress-relieved and normalized specimens. Hardness of the weld zone decreased from as-welded to stress-relieved and normalized specimens. A similar result was observed in the HAZ, but HV values were significantly reduced by the stress-relieved and normalized heat treatments. The HV of the base metals had similar results to those observed in the weld zones. These

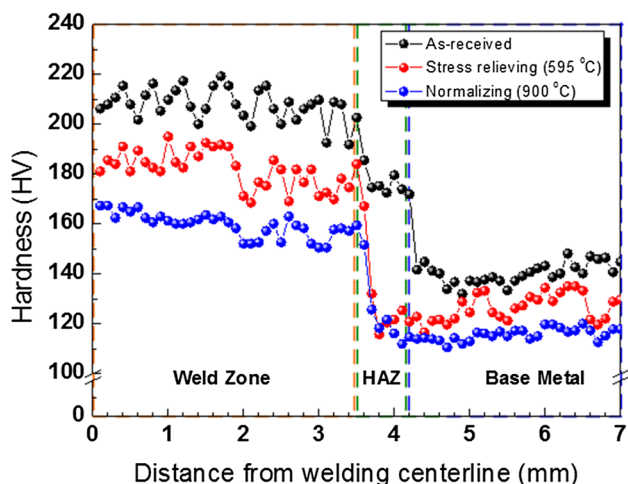


Fig. 9 Vickers hardness (HV) of welded carbon steel pipe from weld metal to base metal

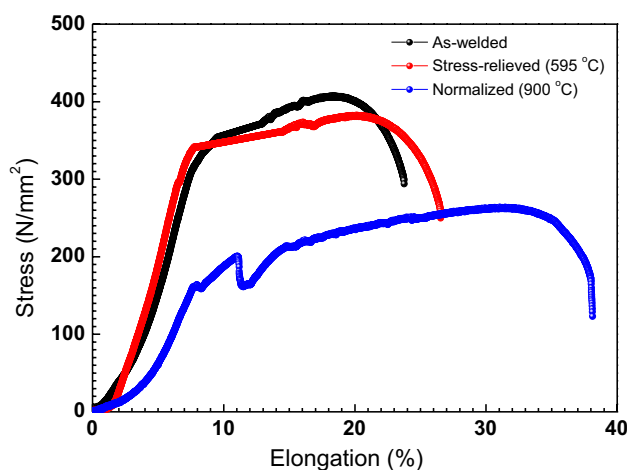


Fig. 11 Results of SSRT for the specimens in the as-welded, stress-relieved and normalized conditions

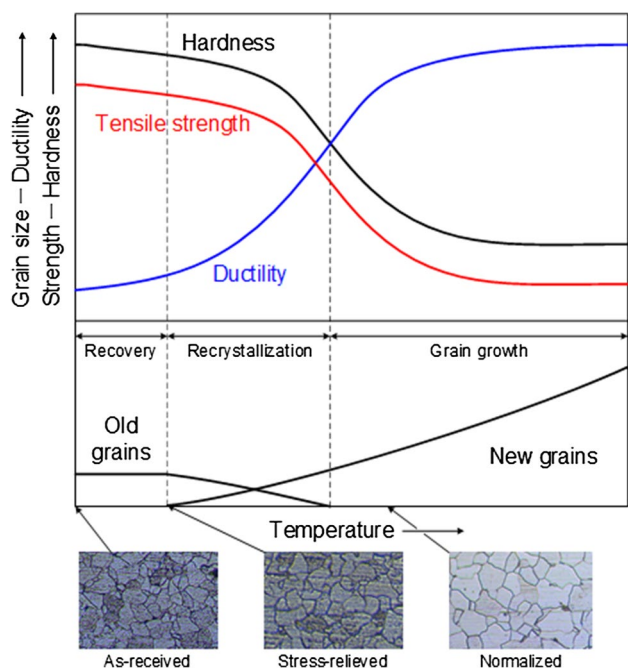


Fig. 10 Schematic representation of the annealing cycle showing the effects on mechanical properties and microstructure according to heat treatment temperature

results are attributed to the microstructure changes caused by the heat treatments. Figure 10 represents the annealing cycle showing the effects of heat treatment temperature on mechanical properties and microstructure. The stress-relieved heat treatment was primarily conducted at a low temperature so that it underwent only the recovery stage. Therefore, the microstructures and mechanical properties of the stress-relieved specimen were not changed significantly. Meanwhile, normalized heat treatments were conducted at a

Table 6 SSRT results of the as-welded, stress-relieved and normalized specimens

Specimens	Yield strength (N/mm ²)	Tensile strength (N/mm ²)	Strain (%)
As-welded	310.80	407.33	23.76
Stress-relieved	296.87	382.33	26.54
Normalized	161.70	263.80	38.12

relatively high temperature, covering from recovery to grain growth stages. Because of the recrystallization and grain growth stages, the microstructures and mechanical properties of the metal changed distinctly in comparison to the as-welded specimen. The grain sizes were determined according to the ASTM E112. The average grain diameters were increased as 1.22 μm, 1.57 μm and 2.20 μm in the following order: as-welded, stress relieved, normalized conditions. From the weld metal to the base metal, the overall decrease in hardness caused a decrease in strength of the normalized specimen and the grain growth had the positive effect on the ductility of the normalized specimen.

3.4 Resistance of SCC

SSRT was conducted to evaluate the resistance to environmentally induced cracking (EIC) in welded carbon steel due to PWHT. The stress–strain curve measured by SSRT is shown in Fig. 11, and mechanical properties for each specimen are listed in Table 6. Yield strength (YS) and tensile strength (TS) of the specimens decreased in the following order: as-welded, stress-relieved, normalized. On the other hand, strain showed the opposite behavior. These results are consistent with the variations of HV in welded specimens as

shown in Fig. 10. The microstructure and hardness changes due to heat treatment lead to these mechanical changes in welded specimens. Thus, the YS and TS were reduced by applying PWHT, but ductility was increased significantly. Therefore, if the reduced YS and TS due to PWHT satisfy the design stress, welded carbon steel pipe with PWHT will have improved service life. Fracture surfaces after SSRT are shown in Fig. 12, and magnified images are shown in Fig. 13. Cup-and-cone ductile fractures with dimple structures were observed on all specimens. The dimple size of the as-received specimen (Fig. 13a) was equal to that of the stress-relieved specimen (Fig. 13b), but larger dimples were observed on the normalized specimen (Fig. 13c). Brittle fracture of the welded carbon steel pipes did not occur in the district heating water solution. Also, if the reduced strength due to PWHT satisfies the design stress, the resistance of specimens to stress corrosion cracking increases in the following order: as-received, stress-relieved, normalized.

4 Conclusions

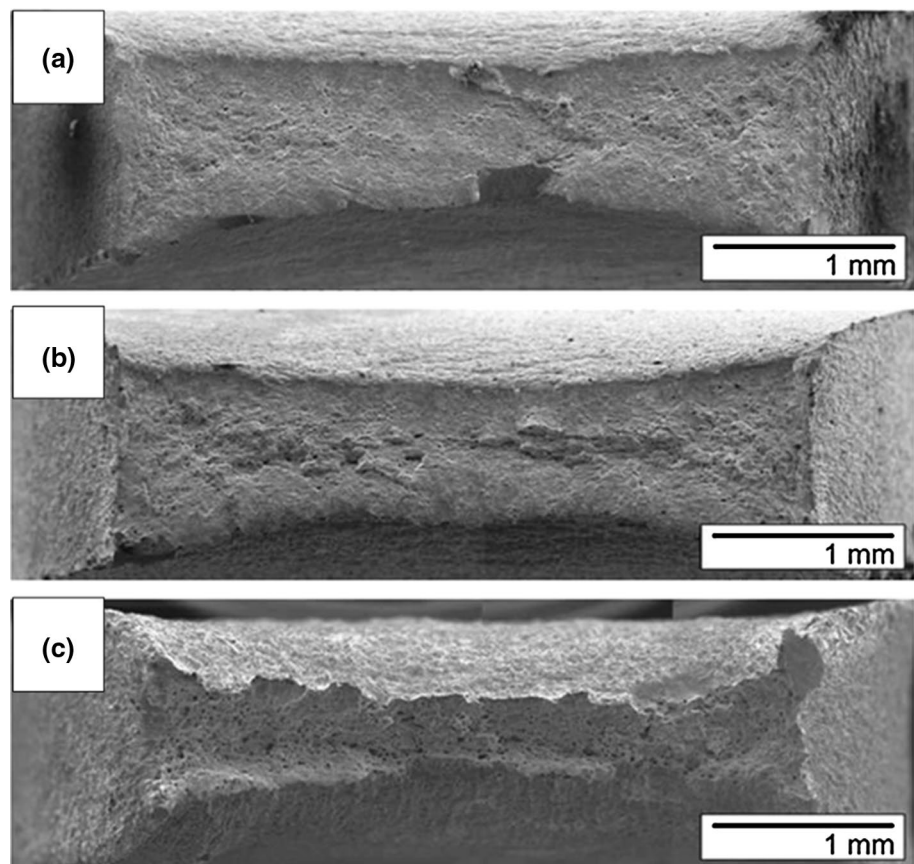
This study investigated the effects of PWHT on the mechanical, electrochemical properties, and resistance to SCC of welded carbon steel pipe. Microstructure

observation, mechanical test, electrochemical test, and SSRT with applying the anodic potential lead to the following conclusions:

1. The stress relieving heat treatment did not cause significant changes in the microstructures of welded carbon steel, but the normalizing heat treatment caused large changes. GF, AF and WF microstructures were observed on the as-welded and stress-relieved specimens, especially in the weld metal, but phase transformations to EF and P occurred as a result of the normalizing heat treatment.
2. The corrosion rate of welded carbon steel specimens was slightly increased by PWHT.
3. HV, YS and TS values decreased, but ductility increased, due to PWHT, with the largest effects observed on the normalized specimen.
4. SSRT indicated that resistance to stress corrosion cracking increased by PWHT, with the largest effect in the normalized specimen although the corrosion resistance of welded carbon steel was decreased by PWHT.

Therefore, the results indicate that welded carbon steel pipe is able to decrease the probability of failure caused by SCC within service life in welded pipeline by normalized

Fig. 12 SEM images after SSRT for the welded specimens: **a** as-welded, **b** stress-relieved, **c** normalized



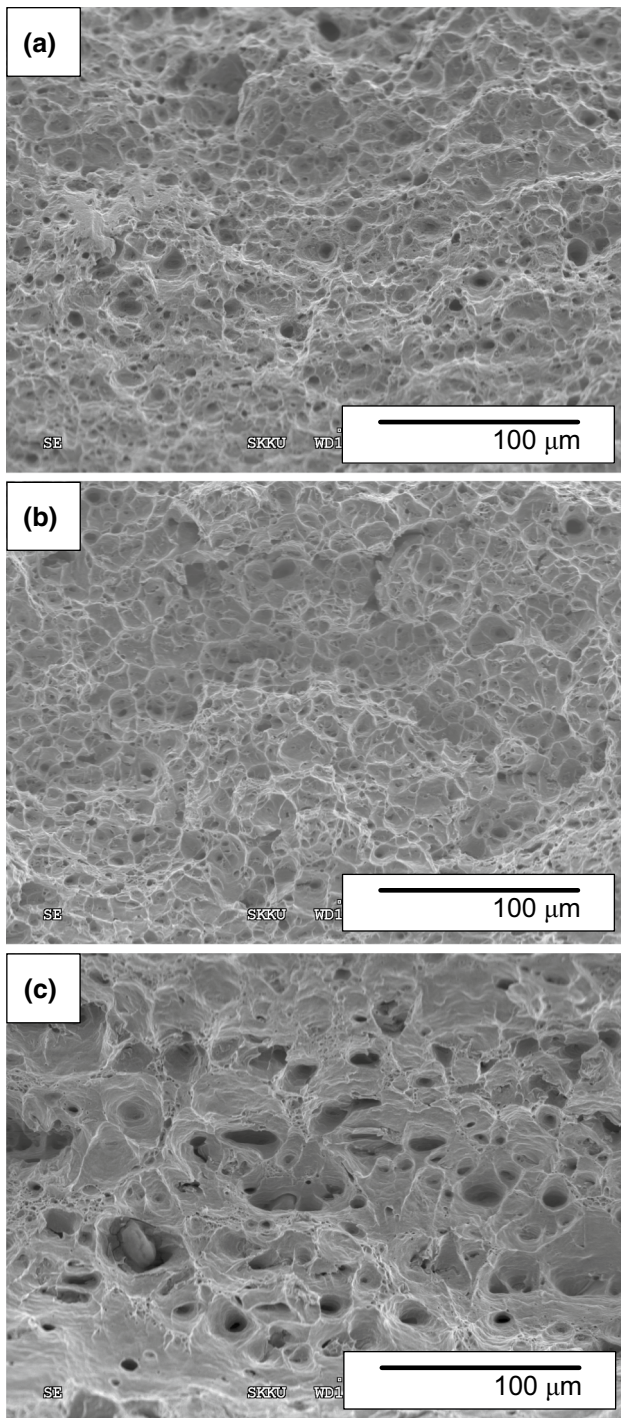


Fig. 13 Magnified SEM images after SSRT for the welded specimens: **a** as-welded, **b** stress-relieved, **c** normalized

treatment if the reduced strength due to PWHT satisfies the design stress criteria.

Acknowledgements This research was supported by the Korea District Heating Corporation (No. 0000000014524).

References

1. M. Protić, S. Shamshirband, D. Petković, A. Abbasi, M.L.M. Kiah, J.A. Unar, L. Živković, M. Raosa, *Energy* **87**, 343–351 (2015)
2. O.K. Kwon, D.A. Cha, C.S. Park, *Energy* **57**, 375–381 (2013)
3. Z. Tang, S.K. Hong, W. Xiao, J. Taylor, *Corros. Sci.* **48**, 322–342 (2006)
4. P.R. Roberge, *Corrosion Inspection and Monitoring* (Wiley, New Jersey, 2007), pp. 1–26
5. L. Garverick, *Corrosion in Petrochemical Industry* (ASM International, Novelt, 1994), pp. 113–121
6. J. Gutzeit, R.D. Merrick, L.K. Scharfstein, *ASM Metals Handbook*, vol. 13C (ASM International, Novelt, 1987), pp. 1262–1287
7. F. Nasirpouri, A. Mostafaei, L. Fathyunes, R. Jafari, *Eng. Fail. Anal.* **40**, 75–88 (2014)
8. F. Daneshvar-Fatah, A. Mostafaei, R. Hosseinzadeh-Taghani, F. Nasirpouri, *Eng. Fail. Anal.* **28**, 69–77 (2013)
9. A. Mostafaei, S.M. Peighambari, F. Nasirpouri, *Eng. Fail. Anal.* **28**, 241–251 (2013)
10. M. Shirinzadeh-Dastgiri, J. Mohammadi, Y. Behnamian, A. Eghlimi, A. Mostafaei, *Eng. Fail. Anal.* **53**, 78–96 (2015)
11. B.K. Srivastava, S.P. Tewari, J. Prakash, *Int. J. Eng. Sci. Technol.* **2**, 625–631 (2010)
12. Q. Xue, D. Benson, M.A. Meyers, V.F. Nesterenko, E.A. Olevisky, *Mater. Sci. Eng.* **A354**, 166–179 (2003)
13. J.E. Ramirez, S. Mishael, R. Shockley, *Weld. J.* **84**, 113–123 (2005)
14. E.I. Samuel, B.K. Choudhary, K.B.S. Rao, *Mater. Sci. Technol.* **23**, 992–999 (2007)
15. M.R. Tavakoli Shoushtari, M.H. Moayed, A. Davoodi, *Corros. Eng., Sci. Technol.* **46**, 415–424 (2011)
16. G. Taniguchi, K. Yamashita, *Kobelco Technol. Rev.* **32**, 33–39 (2013)
17. S.-J. Kim, K.-M. Moon, *Met. Mater. Int.* **4**, 395–401 (2002)
18. S.-J. Kim, S.-K. Jang, J.-I. Kim, *Met. Mater. Int.* **11**, 63–69 (2005)
19. B.K. Srivastava, S.P. Tewari, J. Prakash, *Int. J. Eng. Sci. Technol.* **2**(4), 625–631 (2010)
20. S. Kim, J. Lee, B. Hwang, C.G. Lee, C. Lee, *Met. Mater. Int.* **17**, 137–142 (2011)
21. K.-M. Moon, M.-H. Lee, K.-J. Kim, S.-J. Kim, *Surf. Coat. Technol.* **169–170**, 675–678 (2003)
22. D.A. Jones, *Principles and Prevention of Corrosion*, 2nd edn. (Prentice-Hall, New Jersey, 1996), pp. 143–167
23. B. Craig, *ASM Handbook*, vol. 13A (ASM International, Novelt, 2003), pp. 878–884
24. C.G. Lee, X. Wei, J.W. Kysar, J. Hone, *Science* **321**, 385–388 (2008)
25. G.E. Linnert, *Welding Metallurgy: Carbon and Alloy Steels* (American Welding Society, Miami, 1994), pp. 478–489